Logical on-line hybrid computer actuator and quasi-static testing schemes of PC columns

W.A. Zatar[1] and H. Mutsuyoshi[2]

ABSTRACT | A preliminary investigation of the feasibility of employing Prestressed Concrete (PC) for bridge columns in high seismicity area is conducted. Satisfactory observations encouraged the authors to verify the preliminarily findings by employing a more logical realistic testing technique. A rational on-line hybrid computer actuator testing scheme of seismically vulnerable structures using multi-directional loading is developed. The scheme is utilized for testing three PC column specimens. The innovative findings verified the superior effectiveness of the idea resulting in its recommendation in the latest Seismic Design Code for Prestressed Concrete Structures, Japan. Moreover, for the sake of clarifying and modeling shear strength degradation of such prestressed bridge columns as their drift ratios increase, specimens with low strength ratios are tested using displacement-controlled quasi-static loading. By analyzing the results, an insight of concrete shear strength degradation for PC columns is clarified and modeled.

KEYWORDS | On-line hybrid testing, bridge columns, partially prestressed concrete, quasi-static testing, shear strength, displacement ductility

1 Introduction

The ability of RC columns to withstand a severe earthquake relies mainly on formation of plastic hinges near the column-footing interface. Confining the plastic hinge regions would necessarily enhance the energy dissipation capacities of the RC columns during an earthquake excitation so as to ensure higher values of displacement ductility [1], [2]. Even for ductile members, however, in spite of the energy dissipation capacities, signs of undesirable behavior were frequently reported during previous earthquakes such as the Hyogo-Ken Nanbu 1995 [3]. One unfavorable behavioral sign is the excessive permanent tilting that affects both serviceability and damage recovery of the columns after the earthquake. The overall research objective is to establish a tool that allows a full use of the ductile members with no unfavorable behavioral signs. Therefore, a new technique to examine the feasibility of implementing partially prestressed concrete (PPC) for bridge columns was primarily investigated [4]. The basic idea is to utilize the anticipated advantage of high ductility, encountered in the RC elements, and the reduced permanent displacements and crack control, associated with the PC elements. The authors believe that utilizing the reduced unloading stiffness phenomena of the PC members will much affect the associated permanent displacement. Preliminary investigation, conducted by the authors, utilizing reversed cyclic loading tests resulted in satisfactory findings that

1. D. Eng., Department of Civil Engineering, Raymond Building, University of Kentucky, Lexington, KY40506-0281, USA, E-mail: wael@engr.uky.edu.
2. D. Eng., Dept. of Civil & Environmental Engineering, Saitama University, 255 Shimo-Okubo, 338-8570 Saitama-Shi, Saitama-ken, Japan, E-mail: mutuyosi@mtr.civil.saitama-u.ac.ip

encouraged conduct of this study. A realistic and descriptive testing technique is desired to verify the preliminarily findings. Consequently, one objective of the study is to develop a realistic testing technique that can be employed to verify the feasibility of prestressing the vulnerable bridge columns to enhance their seismic behavior and reduce any undesirable behavioral sign.

Incorporating on-line hybrid computer actuator testing has long been viewed as the most promising testing technique for individual members where severe non-linearities are usually confined to certain plastic hinge regions. The technique, which is developed for multi-directional loading of structures, allows examining the response due to pre-assigned realistic and representative ground motions. Modified excitations of the Hyogo-Ken Nanbu earthquake are used in testing three specimens, as a part of a comprehensive program, and their results are presented. The extensive study included specimens with strength ratios exceeding 1.5, where the strength ratio is defined as the ratio between the shear to flexural capacities. The specimens failed in flexural mode and the concrete strength degradation was not a significant factor to influence the ductility and failure mode. Nevertheless, doubts were raised that the specimens may fail in shear if lower strength ratios are used due to the cyclic effect in decreasing the shear strength. Therefore, another objective of the study is to examine shear strength degradation of the PC columns with low strength ratios as their drift ratios increase.

As a consequence, four specimens with low strength ratios, yet exceed 1.0, were tested using quasi-static loading scheme. The quasi-static loading testing technique allows examining the cyclic effect in the shear strength degradation rather than obtaining the actual response due to an earthquake attack. Interaction of the shear strength and displacement ductility for these PC columns is studied. Applicability of current models, developed for RC bridge columns [5], [6], are examined. Finally, modifications based on experimental findings are proposed to accurately model the interaction of the shear strength and displacement ductility of the PC columns with low strength ratios.

2 On-line hybrid computer actuator testing

On-line hybrid computer-actuator testing (also known as pseudo-dynamic testing) is a computer-controlled experimental technique for structural testing that utilize most types of dynamic loading or earthquake excitations. On-line hybrid computer-actuator test method may be used for structures that are too large, too strong, or too heavy to test on shaking tables while using the same test equipment as in quasi-static cyclic loading tests. Since the method was originated by Hakuno et al. [7], its development and acceptance have been significant. It is finding its way into structural testing because of its efficiency, versatility, and reliability. The name of on-line hybrid describes what happens in the test as the word "hybrid" may mean 1) being a combination of experimental and analytical techniques; 2) being a combination of a computer and load actuators; and finally 3) being a combination of analytical and experimental substructures [8]. In this technique, direct step-by-step time integration is used to solve the equation of motion. The computed displacements at each step are statically imposed on the specimen through computer-controlled actuators in order to measure its restoring forces at the current deformation state. The measured restoring forces are then fed into the equations of motion to compute the next displacement. The numerical time integration process and the on-line loading process are carried out for an entire earthquake ground motion history.

2.1 Background, Concepts and Limitations

In its original development, Hakuno et al. [7] used an electro-magnetic actuator and an analog computer to solve the equation of motion in inelastic earthquake behavior testing model using a real time scale. He noted that there are not as many reversed cycles compared to the loading histories normally used in the cyclic loading tests. The idea was extremely informative but the results were rather poor due to the accuracy

and control limitations of the hardware available at that time. With subsequent developments, Takanashi et al. [9] extended the concept into a more practical form. By implementing a step-by-step numerical time integration scheme to obtain the dynamic response, the on-line loading process can be implemented in extended time scale as a repeated process of loading and computation. The availability of interface devices for analog and digital data conversion has contributed to its wide-spreading. Many researchers have developed variations and applications to structural engineering such as Thewalt and Mahin [10].

Earlier studies utilized linear acceleration integration scheme to solve the equation of motion using measured tangent stiffness [9]. Because of difficulties encountered in testing of stiff systems, the central difference method was adopted. Since that time, it has been considered as the most widely used numerical integration scheme in on-line hybrid testing, especially in Japan. Explicit forms of the numerical integration method such as the central difference, however, result in having the displacement at the current step, which in turn depends on quantities of previous known steps. Any reference of the restoring-force quantity to the current or future time steps, as when formulated using implicit methods, will necessitate approximations or iterative loading schemes [8].

On the other hand, other explicit integration schemes are conditionally stable for small integration time steps resulting in severe limitations of their applications in stiff models or in MDOF systems. Smaller time integration steps will undesirably prolong the test process producing stress relaxation in the loaded specimens. Moreover, considerably small integration time steps may be below the sensitivity and accuracy of the servo-actuators and transducers. The unconditionally stable Newmark method has also been adopted in which the current stiffness is used to estimate the next restoring force, which would incur large errors especially during yielding and unloading sequences. These errors may be minimized by considering very small integration steps and loading to a target near the computed displacement. Shing and Mahin [11] reported on the numerical stability and accuracy of pseudo-dynamic testing.

2.2 Development of A Logical Testing System

In order to physically extend the potential and possibilities of on-line hybrid testing technique, a 3 D.O.F general in-plane loading system is developed. This loading system is capable of imposing independent 3 D.O.F deformation configuration (axial, lateral and rotational deformations) on any test specimen and in response. The corresponding restoring forces are measured based on recommendations of Tanzo et al. [8].

A schematic diagram showing the hardware setup is given in Figure 1. Digital control displacements are sent to 12-bit digital to analog converters (D/A) through a GPIO interface bus, while analog feed back signals are received through an analog to digital converter (A/D). Several other devices such as strain gauges, displacement transducers, loading cells, etc. and other peripherals such as printers, plotters, monitors, drivers, etc. are interfaced through a GPIB bus interface. A workstation to conduct the dynamic analysis is connected to the actuator controller through an interface. Multi-directional deformations are imposed to the specimen through actuators that operate simultaneously. The data are transferred to the actuators through both the D/A and A/D converters, respectively. The realistic pattern of the combined shear, axial and bending loads that the columns commonly undergo can be applied using the proposed system. Briefly, a sequence of loading and feed back process can be described as follows: 1) Actuator displacements are computed based on a desired deformation configuration and then imposed to the specimen; 2) load cells in each respective actuator then measure piston reaction (restoring force) that is employed in the next step.

To overcome the previously mentioned difficulties associated with central difference numerical integration, the so-called mixed (explicit-implicit) integration method was found to suit the on-line hybrid testing. The Operator Splitting (OS) method, the most effective

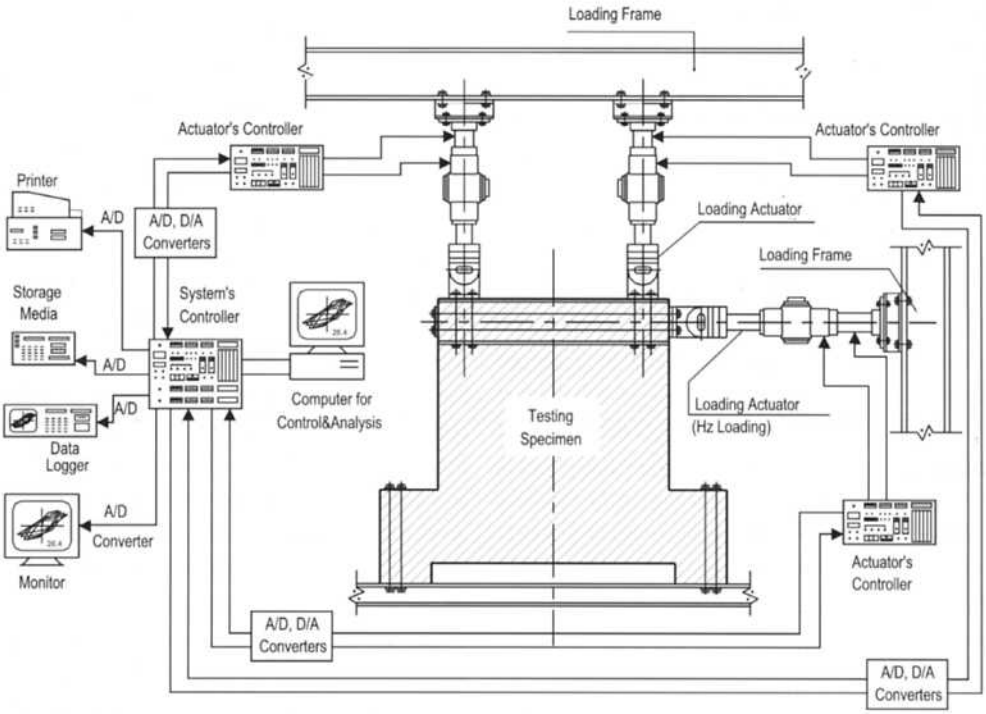

Figure 1. Schematic diagram showing the hardware setup of on-line hybrid testing

technique in terms of both solution stability and accuracy [8], is employed herein. To ensure numerical stability, the time interval *(dt)* is taken as 0.0025 sec. A simplified flowchart of the on-line hybrid testing scheme is shown in Figure 2 and the equations required to calculate the corrector displacements in the next step are:

$$M \cdot a_{n+1} + C \cdot v_{n+1} + K^{I}_{n+1} \cdot x_{n+1} = F_{n+1} \quad \text{.....(1)}$$

$$x_{n+1} = x_n + dt \cdot v_n + (dt^2/4) \cdot a_n \quad \text{.....(2)}$$

$$x_{n+1} = x_{n+1} + (dt^2/4) \cdot a_{n+1} \quad \text{.....(3)}$$

$$v_{n+1} = v_n + (dt/2) \cdot (a_n + a_{n+1}) \quad \text{.....(4)}$$

where,

M, C, K = Mass, damping and stiffness matrices
F = Force vector
x, v, a = Displacement, velocity and acceleration vectors
dt = Integration time.
K^I = Elastic stiffness
K^E_{n+1} = Stiffness of non-linear part at the (n+1) step
x_{n+1} = Vector of corrector displacement at the (n+1) step
x_{n+1} = Vector of predictor displacement at the (n+1) step
F_{n+1} = Restoring force

The developed testing system is a generalized technique that may be employed to any structure. The technique is hereinafter implemented in testing the PC columns.

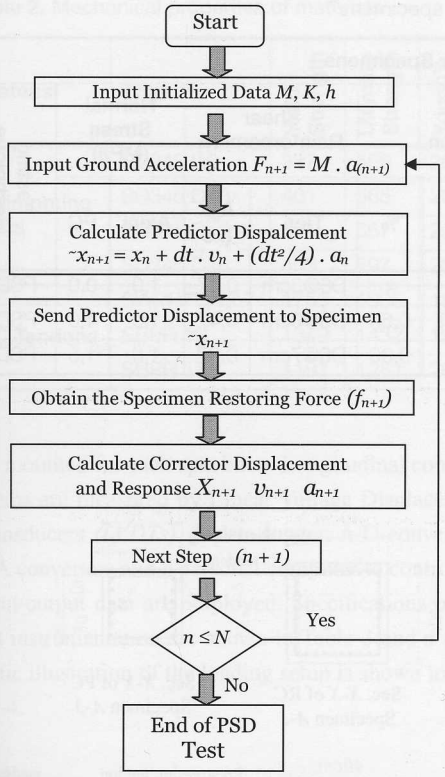

Figure 2. Flow chart showing steps of on-line hybrid tests

3 Testing of PC columns

3.1 Experimental Variables

Three specimens named A-l, A-2 and A-3 are tested using on-line hybrid testing technique. Specimen A-l is a control RC specimen and the other two specimens are PC specimens. Reinforcement, prestressing and shear reinforcement information are given in Table 1. The strength ratios of specimens A-l and A-2 exceed 1.50 to ensure flexural dominant behavior while it is 1.07 for specimen A-3 to represent the case when shear failure, even after flexural yielding, may occur. The other experimental variable is the mechanical prestressing ratio (λ) [4], which is defined as the contribution of the prestressing tendons to the overall cross-sectional capacity, Eq. [5].

$$\lambda = \Sigma(Aps_i.Fp_i) / (\Sigma As_j.Fs_j + \Sigma Aps_i.Fp_i) \quad \text{..... (5)}$$

where:

Aps_i = Area of each prestressing tendon
Fp_i = Stress of each prestressing tendon
As_j = Area of each reinforcing bar
Fs_j = Stress of each reinforcing bar

Specimens

Each specimen consists of a column part cast integrally with a bottom rigid stub (footing). For specimens A-l and A-2, the column and footing dimensions are 40x40x165 cm and 45x60x130 cm, respectively. For specimen A-3, the column and footing dimensions are 30x30x125 cm and 65x60x120 cm, respectively. Dimensions, details and allocation of the strain gauges of the specimens are given in Figure 3. Specimens A-l and A-2 have bi-axial symmetrical reinforcement and prestressing tendons while they are arranged near the extreme tension and compression fibers for specimen A-3 (Figure 3c). Specimen A-l is a control RC specimen with $\lambda = 0.0$ while λ of specimens A-2 and A-3 are 0.64 and 0.30, respectively.

In order to monitor the influence of prestressing of the columns on their behavior, fixation of the stub to a steel base is insured through the use of auxiliary prestressing tendons with another group of strain gauges attached. The response of the columns due the combination of the axial and earthquake loads is monitored. The rigid connection between the footings and the bases disregards the surrounding soil response, which is not the objective of this paper and will be taken care of in future publications. Special grooves prepared at bottom of the footings allow post tensioning. Locations of the strain gauges are chosen to monitor the yield strains and yield penetration near the expected hinge locations [12].

Materials

Ready-mixed normal weight concrete with a 28-day compressive strength of 35 N/mm^2 is used. Ratio of the main reinforcement to the effective area of the cross

Table 1. Details of reinforcing bars and prestressing tendons in specimens*

Specimen No.	Variables of PC Pier Specimens											
	Mechanical Pre-stressing Ratio	Cross Section		Reinforcing Bars & PC Tendons in Cross Section				Shear Reinforcement		Normal Stress (MPa)		Testing Technique
		Dimen-sions	a/d	Re-inforce-ment	%	PC	%	Ties	A_{sh}/ b.s	Axial	PC	
A-1	0,00	40*40 cm	5,43	32D13	2,65	x	x	D6@3cm	0,47	1,0	0,0	PSD*
A-2	0,64	40*40 cm	5,43	16D10	0,79	8 SWPR ϕ 12.7	0,63	D6@3cm	0,47	1,0	4,0	PSD*
A-3	0,30	30*30 cm	4,20	10D16	2,22	2 ϕ 13	0,30	D6@7cm	0,27	1,0	1,5	PSD*

*. Pseudo-dynamic test (On-line Hybrid testing)

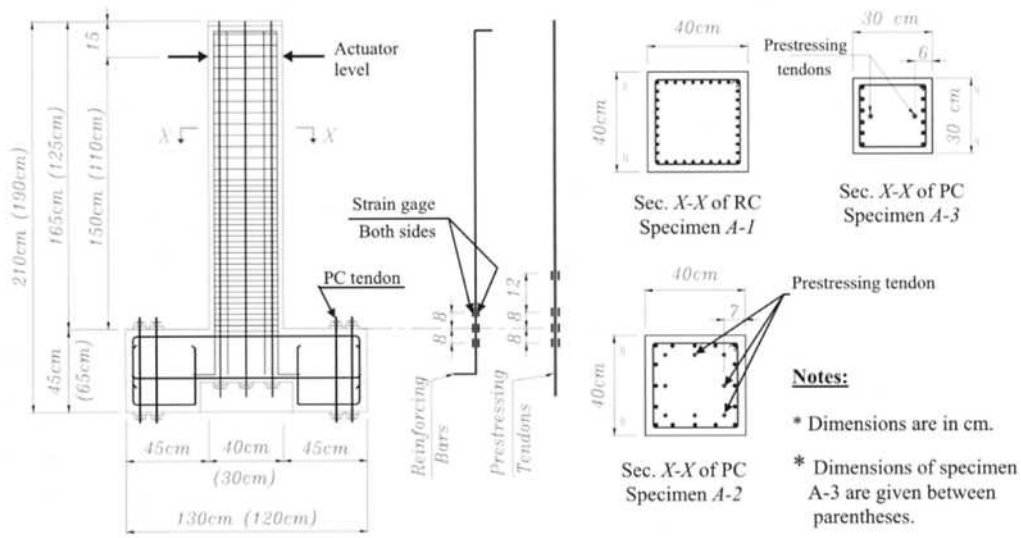

a) Dimensions b) Strain gages c) Cross sections

Figure 3. Details of specimens

section ranges from 0.79 percent to 2.65 percent. Mechanical properties of the reinforcing bars and the prestressing tendons are shown in Table 2. Ratio of the prestressing tendons to effective area of the cross section ranges from 0.0 to 0.63 percent. The prestressing tendons, strand type, are anchored at the top of columns and at the bottom of the footings to avoid undesirable slippage. Volumetric ratio of the ties to the concrete core is 0.47 percent in the lower half of specimens A-1 and A-2 and 0.27 percent for specimen A-3. At the upper half of the columns, percentage of the ties is reduced to 50% of its value at the lower half.

Instrumentation and Loading Setup

Concrete and steel strains at various locations, deflections along the specimen length, axial and lateral loads are monitored during each test through the use of an extensive instrumentation. A total of 44 strain gauges

Table 2. Mechanical properties of materials

Material	Type	Yield Strength	Ultimate Strength	Young's Modulus
Reinforcing Bars	SD345 D6	387	566	206
	SD345 D10	401	565	206
	SD345 D13	391	567	206
	SD345 D16	403	597	202
PC Tendons	SWPR7B 12.7	1753	1935	191
	SBPR 13	1349	1432	198
	SBPR 17	1197	1281	203

are mounted for each specimen. Longitudinal concrete strains are measured by Linear Voltage Displacement Transducers *(LVDTs)*. A data logger, A/D converters, D/A converters and a personal computer to control the input/output data are employed. Specifications of the test instrumentation are shown in Table 3 and a schematic illustration of the loading setup is shown in Figure 4.

Table 3. Specifications of test instrumentation

Hard Part	Specifications
Controlling Computer	Apple Mac. : Quadra 800
AD-DA Converter	National Instruments : Mio-16(H) Voltage = -10.0A, +10.0V Resolution 12bit
Software	National Instruments : LabVIEW 4.01J
Data Logger	Tokyo Sokki : TDS601 Scan Speed = 80 (m/sec)
Actuator	Shimazu : EHF-JB20 Electric Oil Pump Static Capacity = 294 (kN) Dynamic Capacity = 196 (kN) Maximum Stroke = 100 (mm) Precision : Load Full Scale Range = 0.5% Disp. Full Scale Range = 1.0%
Hydraulic Jack	Riken : D5-50 Capacity = 490 (kN)
Load Cell	Tokyo Sokki : KC50B Capacity = 490 (kN)
Oil Pump	Riken : MP-10 Capacity = 8.0A, 70.0 (MPa)
Control Valve	Riken : MRV-PAB Capacity = 10.0A, 70.0 (MPa)
Oil Cooler	Riken : RLT-303 Water 12.0 (L/min)
Sleeves	Riken : CLF-50-A, CLF-50-B Capacity = 490 (kN)
Roller	THK : LR-50134 Static Capacity = 255 (kN) Dynamic Capacity = 149 (kN)

Testing

A damping ratio of 3% is assumed before yielding. No damping is assumed after yielding since hysteretic damping dominates. An axial compression stress level of 1.0 MPa is applied at top of each specimen. The used ground acceleration is the *modified Hyogo-Ken Nanbu 1995 (NS direction)* excitation with a time interval of 0.01 second and a total duration of 14.0 seconds. The time scale is the original one while the maximum input acceleration for each specimen based on *"Design Specifications for Highway Bridges -Part V- Seismic design (1998) "* [13], is as follows:

Assuming a target elastic natural period (T) of 0.3 second, the mass for each specimen can be obtained based on K_E (Eq. [6]). Equivalent lateral force coefficient K_{he} is calculated by Eq. [7]

$$T = 2\pi\sqrt{\frac{M}{K_E}} \quad \text{.....(6)}$$

$$K_{he} = K_{hc}/\sqrt{2\mu - 1} \quad \text{.....(7)}$$

where;

$$K_{hc} = C_z \cdot K_{hco}$$

$$\mu = 1 + (\delta_u - \delta_y)/\alpha\delta_y$$

T = Natural period
K_E = Elastic stiffness
M = Mass (kg)
K_{he} = Equivalent lateral force coefficient used with the ductility design method
K_{hc} = Design lateral force coefficient
μ = Allowable ductility factor

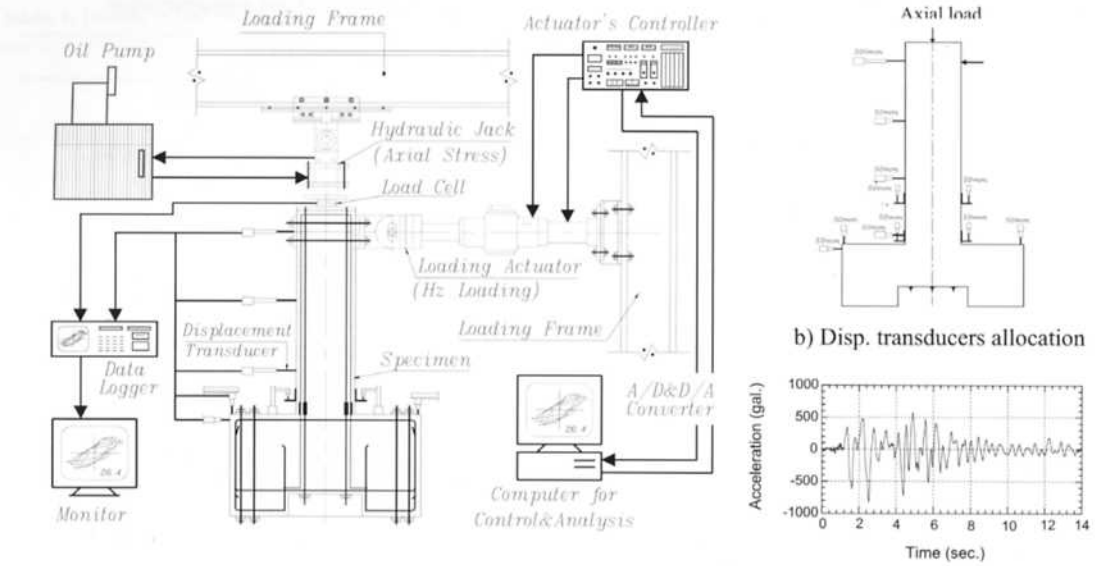

a) Loading setup and instrumentation

b) Disp. transducers allocation

c) Input acceleration

Figure 4. Experimental loading setup, displacement transducers allocation and the Hyogo-ken Nanbu input acceleration

K_{hco} = Standard value of type I design lateral force coefficient = 2.0 (dependent on T and ground classification)

C_z = Zone Modification factor (=1.0)

δ_u = Yield displacement, which is defined as the displacement corresponding to the intersection of extrapolating the stiffness after cracking and the stiffness after yielding on the load-displacement curve

δ_y = Ultimate displacement, which is defined as the displacement when the load degrades to 80% of its previous maximum value on the load displacement curve

Assuming $\delta_u = 5\delta_y$ *and* $\alpha = 1.5$ results in $\mu = 3.67$ and $K_{he} = 0.8$. The coefficient a_m is then obtained from Eq. [8] based on the mass and the yielding lateral load. The maximum input earthquake acceleration (α_{input}) for each specimen is obtained from Eq. [9] based on $\alpha_{max.}$ = the original 818 *gal* of the earthquake. Therefore, The resulting maximum input earthquake accelerations for specimens A-l, A-2 and A-3 are 563, 474 and 1227 gal, respectively (Table 4).

Table 4. Variables of on-line hybrid testing

Specimen	Mass (t)	Initial Stiffness (MN/m)	Input Acceleration (gal)	Time Scale
A-1	37.8	16.6	563	1.00
A-2	36.7	16.1	474	1.00
A-3	18	13.8	1227	0.50

$$\alpha_m = P_e / M \quad (8)$$

$$\alpha_{input} = \alpha_{max.} \cdot \alpha_m / (K_{he}\, G) \quad (9)$$

4 Test results and discussion

The behavior of each specimen is presented graphically in the form of a hysteretic column shear force versus tip deflection relationship and time histories for displacement, acceleration and velocity. Figure 5 shows the hysteretic load-displacement curve of the RC specimen A-l. The maximum displacement is 10.5

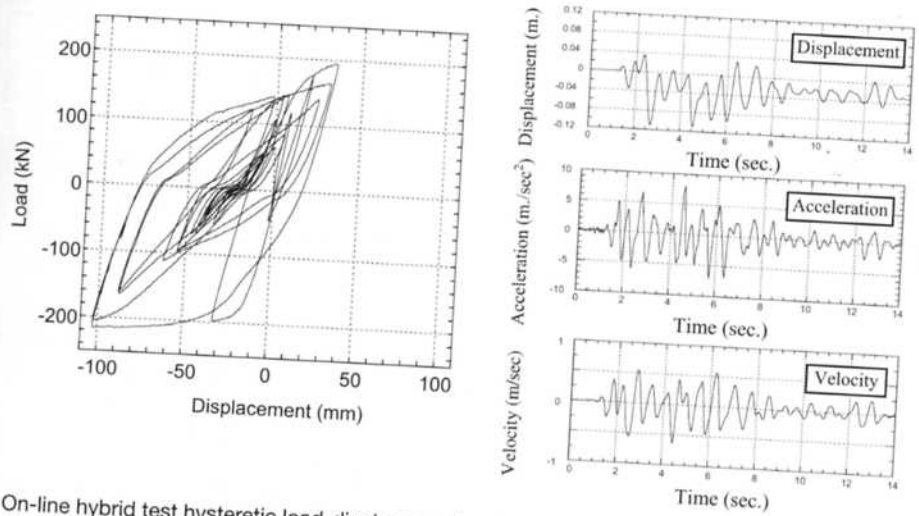

Figure 5. On-line hybrid test hysteretic load-displacement curve and time histories of RC specimen A-1

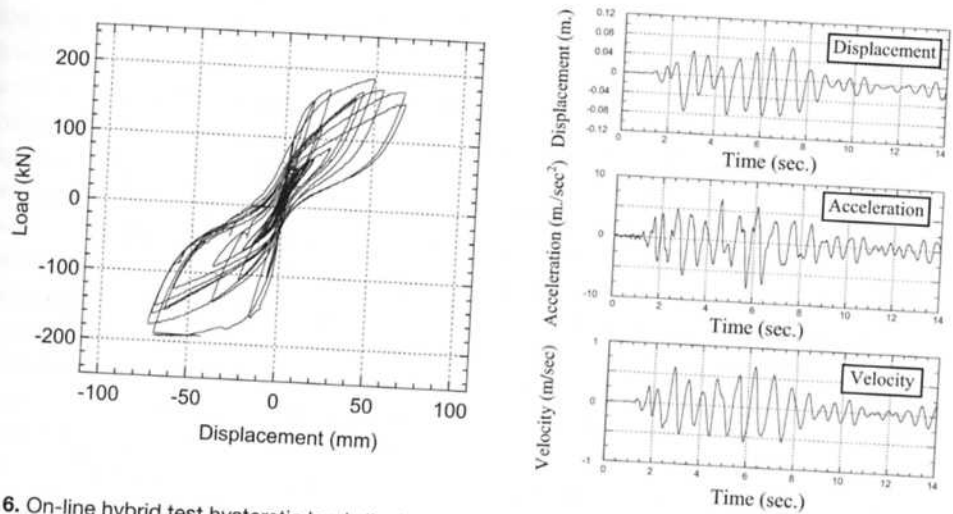

Figure 6. On-line hybrid test hysteretic load-displacement curve and time histories of PC specimen A-2

times the yielding displacement (δ_y) in the left side of the plot and 3.6 δ_y in the right side, showing that the deformations are drifting in the negative direction of the plot. High hysteretic energy is dissipated during the excitation. A maximum displacement of -0.11 m in the negative side is recorded and eventually a permanent shift of -0.025 m is observed. Figure 6 shows the load-displacement curve of specimen A-2. Stiffness degradation during unloading and pinching [6] are clear in both directions of loading. The maximum displacement is 6.63 δ_y in the left side of the plot and 6.30 δ_y in the right side. For ductility considerations of PC column and since there are no clear yielding point, the yielding point is defined as the intersecting point of extrapolating the stiffness after cracking and the stiffness after yielding. Hysteretic energy is less than that of the comparable RC specimen A-l. Flexural crack widths are smaller than those of specimen A-l since

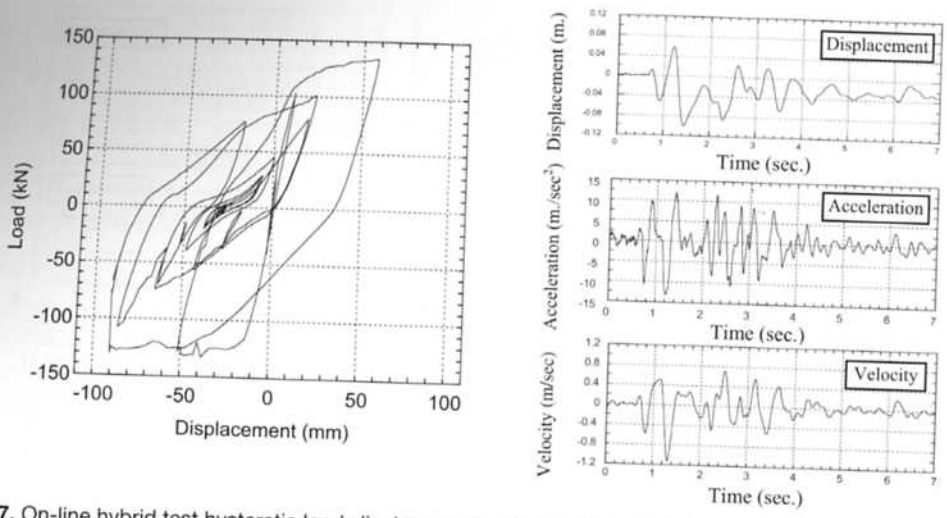

Figure 7. On-line hybrid test hysteretic load-displacement curve and time histories of PC specimen A-3

residual tensile forces in the PC tendons enabled to close previously opened cracks, which is an advantage of prestressing bridge columns. A maximum displacement of -0.075 m is recorded. Almost no shift of the response in the negative side is observed resulting in much smaller permanent displacement than specimen A-l, and may be considered as the main merit of using PC columns. Figure 7 shows the hysteretic load-displacement curve of specimen A-3. Maximum displacements of 7.35 δ_y and 3.75 δ_y are recorded in the left and right side of the plot. The hysteretic energy is slightly less than that of the RC specimen A-l. Though shear cracks were apparent, the overall hysteretic behavior of specimen A-3 is, more or less, not different from that of specimen A-l because of the associated low mechanical prestressing ratio of specimen A-3. A maximum displacement of -0.075 m and a shift of the response in the negative side are observed. A permanent displacement of -0.02 m, which is a bit smaller than specimen A-l is observed.

In conclusion, the test results displayed that neither a biased response nor a permanent drift is anticipated for the prestressed concrete bridge columns under excitations with the nature of the Hyogo-ken Nanbu earthquake. At the mean time, smaller widths of the residual cracking at the bottom end of the columns than those of the RC columns are anticipated. The innovative findings of the feasibility associated with employing prestressing to bridge columns shows a superior effectiveness to enhance the seismic behavior of the vulnerable columns and reduce any undesirable behavioral signs. Such an enhancement, in turn, encouraged its recommendation in the latest Seismic Design Code for Prestressed Concrete Structures, Japan [13].

Moreover, since the other objective of the study is to clarify and model the degradation of shear strength of PC bridge columns as the response increases, an additional experimental program that includes 4 specimens with relatively low strength ratios is conducted. The specimens are tested using displacement controlled quasi-static scheme as shown hereinafter.

5 Displacement controlled quasi-static testing

5.1 Specimen Variables

Four specimens named E-l through E-4 with low strength ratios are tested. The specimens have identical dimensions to those of specimen A-3 in Figure 3. Variables of the test specimens are shown in Table 5 while

Table 5. Specimens with low strength ratios

Specimen No.	Variables of PC Pier Specimens										
	Mechanical Pre-stressing Ratio	Cross Section		Reinforcing Bars & PC Tendons in Cross Section				Shear Reinforcement		Normal Stress (MPa)		Testing Technique
		Dimen-sions	a/d	Re-inforce-ment	%	PC	%	Ties	A_{sh}/ b.s	Axial	PC	
E-1	0.00	30*30 cm	4.20	12D16	2.68	---	---	D6@7cm	0.27	1.0	0.0	Quasi-static
E-2	0.30	30*30 cm	4.20	10D16	2.22	2 ϕ 13	0.30	D6@7cm	0.27	1.0	1.5	Quasi-static
E-3	0.21	30*30 cm	4.20	12D16	2.68	2 ϕ 13	0.30	D6@5.5cm	0.34	1.0	1.5	Quasi-static
E-4	0.37	30*30 cm	4.20	10D16	2.22	2 ϕ 13	0.50	D6@5.5cm	0.34	1.0	3.0	Quasi-staic

the cross-sectional detailing is, more or less, similar to specimen A-3. Specimens are designed to possess low strength ratios in order to facilitate monitoring the shear strength degradation and its effect on the overall response. Exceeding unity and ranged from 1.07 to 1.18, the strength ratios of the specimens are chosen to study their effect on the resulting failure though the shear failures are not anticipated to occur before flexural yielding of the longitudinal reinforcing bars. Tests by Zatar and Mutsuyoshi [4] for PC columns with higher strength ratios showed that the shear strength degradation is delayed thus implying the significant role that the strength ratio plays in controlling the shear degradation, the behavior and the final failure mode. The strength ratios were calculated by changing the shear reinforcement and the prestressing level. The 1st specimen (E-l) was a control RC specimen while the other three specimens were PC specimens with λ ranged from 0.0 to 0.37. Nominal compressive strength of the concrete is 35 MPa and other material properties are shown in Table 2.

Testing Setup

The specimens are mounted vertically and are loaded horizontally through a loading actuator. The experimental loading setup is, more or less, similar to that of the online hybrid testing except that the computer is only used for control purposes rather than analysis. Full description and instrumentation can be found elsewhere [4]. Pre-determined increasing displacement amplitudes are fed to the specimens during testing. The first displacement amplitude is the cracking displacement followed by the first yielding displacement. Then, consecutive multiple integers of the yielding displacements are applied until failure of the specimens occurred.

5.2 Hysteretic Load-Displacement Relationships

As anticipated, the higher the mechanical prestressing ratios, induced through addition of the prestressing tendons to the control specimen, the higher the load carrying capacities. Figure 8a shows the load-displacement curve of the control RC specimen E-l with a strength ratio of 1.18. Pinching of the hysteretic behavior is noticeable due to shear and strength degradation, and is pronounced at a drift angle (δ) = 0.047 due to a final shear failure mode after yielding of the reinforcing bars. Figure 8b shows the load-displacement curve of the PC specimen E-2 with $\lambda = 0.3$ and a strength ratio of 1.07. Although the strength ratio is smaller than that of specimen E-l, no pinching is observed. The strength degradation commences at a higher drift ratio than that of specimen E-l followed by a final shear failure mode. The reduced pinching of specimen E-2 supports the opinion associated with the role of prestressing in increasing the shear strength of bridge columns. Figure 8c shows the load-displacement curve of the PC specimen E-3 with $\lambda = 0.21$ and a strength ratio of 1.14. Three repetitions of each cyclic displacement were used for specimen E-3 to magnify the significance of

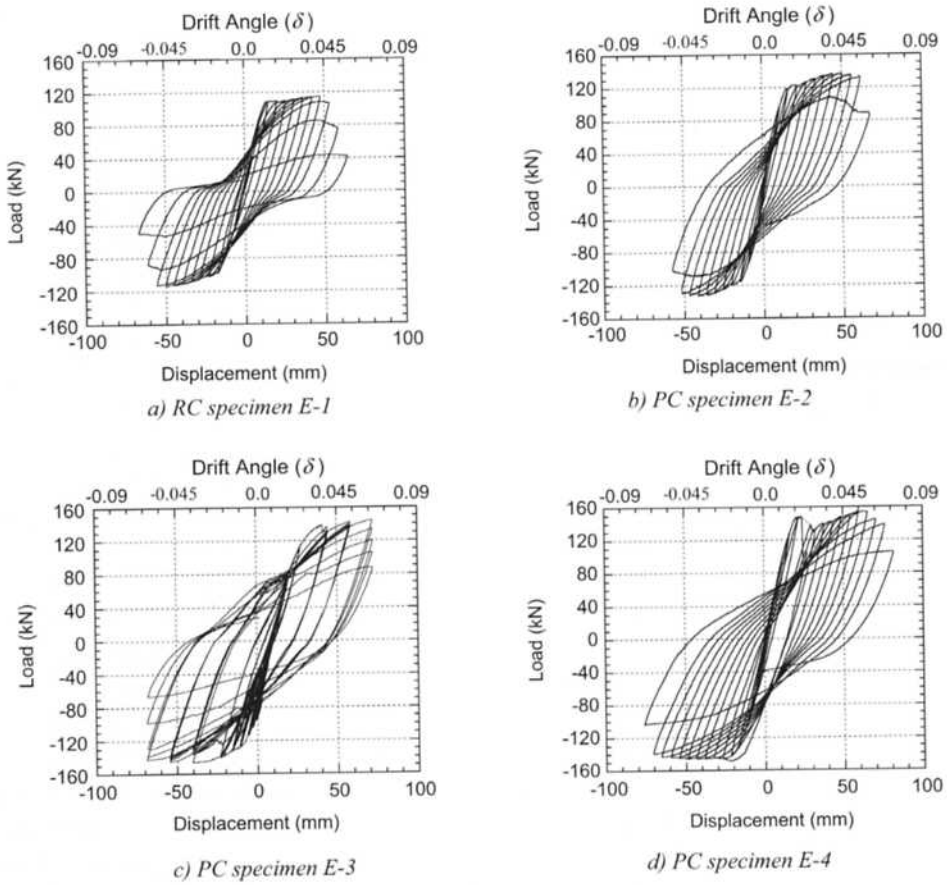

Figure 8. Hysteretic load-displacement curves of specimens

strength degradation due to repeated, yet equal, cyclic displacement amplitudes. The strength degradation leading to a shear failure after flexural yielding commences at $\delta = 0.064$. Figure 8d shows the load-displacement curve of the PC specimen E-4 with the highest λ of 0.37 and a strength ratio of 1.11. Almost, no pinching is observed. The strength degradation after flexural yielding of the prestressing tendons is observed at $\delta = 0.064$, followed by a final shear failure.

It can be observed that slight decreases in the strength ratios of the PC specimens than that of the control RC specimen do not necessarily lead to shear failures at displacement amplitudes smaller than that of the RC specimen since the overall shear capacity is enhanced by prestressing. An overview of the concrete shear strength degradation as a result of the cycling effect that usually that results from an earthquake excitation is shown hereafter.

6 Ductility and shear strength interaction

Examination of bridge columns in earthquakes enables a clear distinction to be made between brittle modes of failure and ductile shear failure, where the ductility allows developing hinges before shear failure occurs. Therefore, it is necessary to inhibit shear modes of failure by increasing the strength ratios [1]. This is acknowledged in the conceptual model for shear strength proposed by the *ATC-Seismic Design 1981*

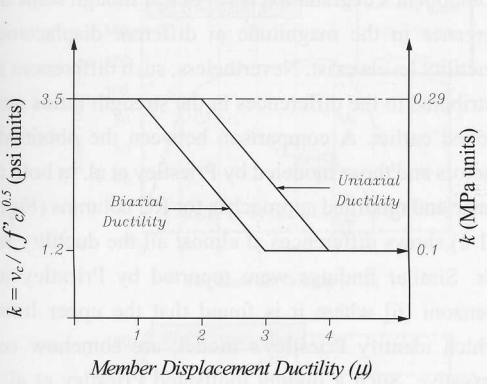

a) Model by Priestley et al.

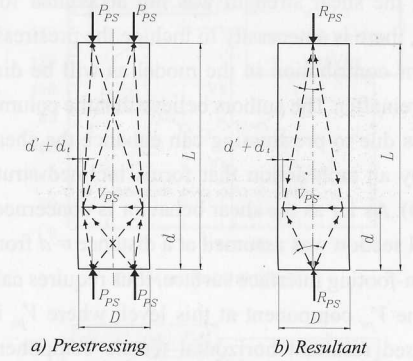

a) Prestressing b) Resultant

Struts & tie for individual external prestressing

Strut-tie model for resultant of prestressing forces

b) A Truss model for prestressing component

Figure 9. Model of concrete shear strength factor versus ductility by Priestley et al. and a truss model for prestressing component of shear strength

[14]. In this model, the shear strength is assumed to decrease in a linear fashion as the member displacement ductility increases. If the shear force corresponding to the flexural strength is less than the residual shear strength, a ductile flexural response is ensured. If it is greater than the initial shear strength, a brittle shear failure results. If the shear force is between the initial and the residual shear strength, the shear failure occurs at a ductility corresponding to the intersection of the strength and force-deformation characteristics. Although this behavior is reasonably well accepted, it has not found its way into concrete design codes, except in very few codes with no explicit relationship between ductility and shear strength [5]. The *AIJ* recommendations proposed that for a ductile member, the permissible diagonal compressive stress is progressively reduced as the plastic rotation increases [15], which is somehow similar to the *ATC* model. Nevertheless a shortcoming of the *AIJ* is that its recommendations are proposed only for rectangular sections.

6.1 Model by Priestley et al.

Recently, a considerable experimental research for RC columns has been directed towards a better definition of the shear strength/ductility relationship. Additional results from Priestley et al. [16] and [17] have supplemented this data. Furthermore, Priestley and Benzoni [6] refined previous models proposed by Ang et al. [14] The model by Priestley and Benzoni [6] is shown to be accurate enough to a full range of experimental database. Priestley et al. [5] verified the superior accuracy of his proposed model over other models. Additionally, Priestley and Benzoni [6] presented modifications of the original model to account for special cases of RC columns. In the approach by Priestley et al. [5] for RC columns, the components of the overall shear resistance are separated in the form of steel truss component (Vs), axial force component (V_p) and concrete component (V_c). The magnitude of V_s depends on the transverse reinforcement content. The V_p component depends on the column aspect ratio. The concrete component (V_c) is equal to $k \,.\, (f'_c \,.\, A_e)^{0.5}$ where k depends on the level of ductility (Figure9a) and A_e is the effective shear area = $0.8\, A_g$, where A_g is the gross sectional area.

6.2 A Proposed Model for PC Columns with Low Strength Ratios

Since the model by Priestley et al. was mainly proposed for RC columns and never dealt with PC columns, the effect of the prestressing tendons in

increasing the shear strength was not accounted for. Therefore, there is a necessity to include the prestressing tendons contribution in the model as will be displayed hereinafter. The authors believe that the column axial stress due to prestressing can enhance the shear strength by an arch action that forms inclined struts (Figure 9b). As far as the shear behavior is concerned, the critical section was assumed at a distance = d from the column-footing interface surface, thus requires calculating the V_{ps} component at this level, where V_{ps} is the proposed resultant horizontal tensile component due to the axial prestressing. In the proposed model, individual prestressing tendons may participate in enhancing the overall shear strength through formation of individual compression struts. A simple calculation method is implemented through identification of the resultant (R_{ps}), where $R_{PS} = \Sigma P_{PS}$. The magnitude and point of application of the external applied prestressing forces are calculated from statics. By solving the equilibrium truss mechanism in Figure 9(b), the forces in the inclined struts as well as the required resultant horizontal tensile component V_p are obtained. Finally, the overall shear resistance is composed of the summation of the four components V_c, V_S, V_p *and* V_{ps} *as* shown in Eq. [10].

$$V = V_c + V_s + V_p + V_{ps} \quad \text{.....(10)}$$

6.3 Justification of Methodology

During testing of each specimen, strains in the reinforcing ties are digitally recorded and the associated stresses are obtained. Using these stresses and the determined inclination angle of the major shear crack, the V_s component could be experimentally obtained at different loading stages. Calculating V_p and V_s and subtracting from the experimental lateral loads at each loading stage, the V_c component is calculated. Figure 10 shows a comparison between the experimental components of the shear resistance of all specimens. From the V_c component, the k factors are calculated and plotted versus the displacement ductility. It can be seen From Figure 10 that the assumed principal of the V_c component's degradation is very clear though some differences in the magnitude at different displacement ductility levels exist. Nevertheless, such differences are attributed to the differences in the strength ratios mentioned earlier. A comparison between the obtained k factors and those modeled by Priestley et al. in both the basic and modified approaches for RC columns (Figure 11 a) shows differences at almost all the ductility levels. Similar findings were reported by Priestley and Benzoni [6] where it is found that the upper limits, which identify Priestley's model, are somehow conservative. Such a finding motivated Priestley et al. to modify the model as shown in Figure 11a.

In order to have a better simulation of the obtained experimental k values than those obtained by Priestley's et al. approach, a modification in the model is proposed herein to account for cases of PC columns with low strength ratios. The proposed model, shown in Figure 11b, assumes that an initial value of 0.2 is to be used as the k value (if MPa units are used) up to a displacement ductility of 2.0 followed by a gradual degradation of the k factor when increasing the displacement ductility up to 4. Then, a constant k value of 0.1 is used up to a displacement ductility of 5.0 followed by a gradual decrease in the k value till it vanishes at a displacement ductility of 6.0. It should be noted that, opposite to Priestley's model, the k factor vanishes in the proposed model because this model is intended for PC columns with low strength ratios. It might be expected that for PC columns with higher strength ratios, the k factor might have a value rather than zero for a displacement ductility of more than 6. Nevertheless, such expectation requires further experimental verification, and is out of the scope of this investigation.

7 Conclusions

In order to develop and apply a logical and descriptive testing technique to verify the feasibility and effectiveness of prestressing of vulnerable bridge columns to enhance their seismic behavior and reduce any undesirable behavioral sign, a rational on-line hybrid com-

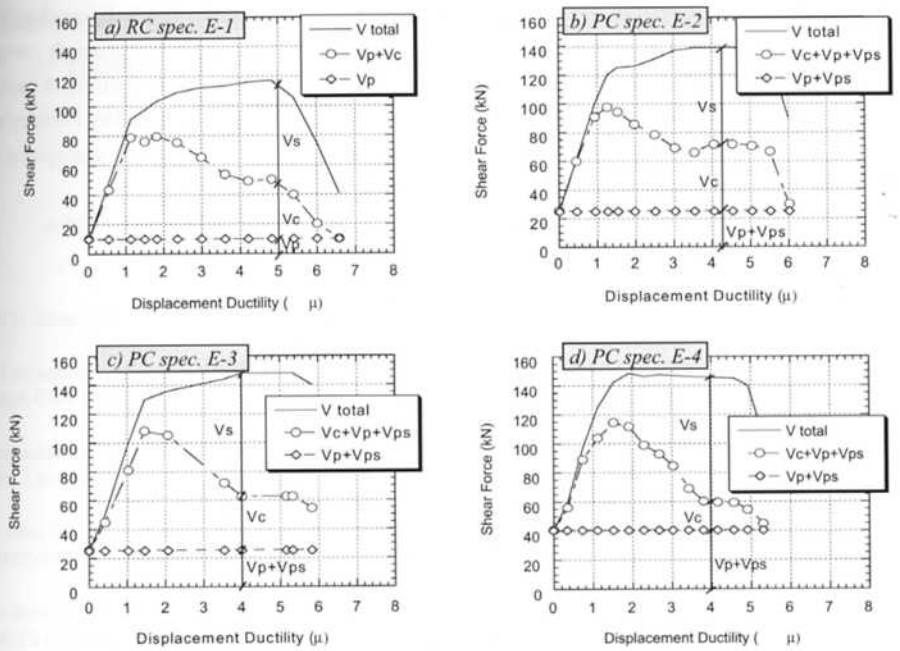

Figure 10. Displacement ductility versus shear strength components

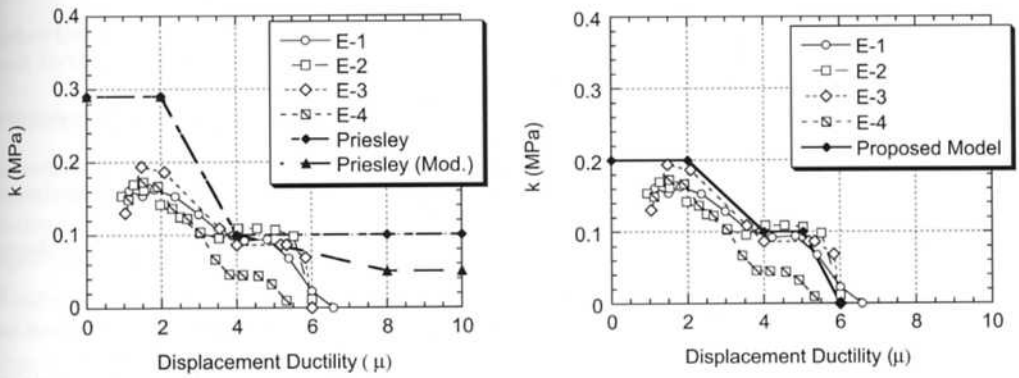

a) Experimental and Priestley's et al. k factors

b) Proposed k factors versus displacement ductility

Figure 11. Experimental and Priestley's et al. *k* factors versus displacement ductility and justification of the proposed *k* factors versus displacement ductility

puter actuator testing scheme for multi-directional loading is developed. The scheme is utilized for testing three PC column specimens. The innovative findings showed the superior effectiveness of the idea thus encouraged its recommendation in the latest Seismic Design Code for Prestressed Concrete Structures, Japan.

In order to clarify and model the cyclic effect on the shear strength of prestressed concrete bridge columns, specimens with low strength ratios are tested using dis-

placement-controlled quasi-static testing technique. It is experimentally verified that the concrete shear strength degrades as a result of increasing the displacement ductility. The interaction between the concrete component of the shear resistance and the displacement ductility is clarified. Examination of Priestley's et al. model, originally developed for RC columns, for prestressed bridge columns displayed an exaggeration of estimating the concrete shear strength component especially at high displacement ductility. A model that is based on the principals presented by Priestley's et al., with modifications for PC columns, is proposed and its applicability is verified.

REFERENCES

[1] Priestley, M. J. N., Seible, F., and Calvi, G., M., Seismic design and retrofit of bridges, John Wiley & Sons Inc, 1996.

[2] Design Specifications of Highway Bridges, Part V: Seismic Design, Earthquake Disaster Prevention Research Center, Public Works Research Institute *(PWRI) FED Report No. 9801,* Japan, 1998.

[3] Takeda, S., Okimura, T., and Lee, T. Y.: '*Seismic motion and damage characteristics'. Preliminary Report on the Great Mansion Earthquake* by Japan Society of Civil Engineers, 1995, pp.270-286.

[4] Zatar, W., and Mutsuyoshi, H., '*Control of residual displacements of RC piers by prestressing'. ASCE (American Society of Civil Engineers) Publication,* ISBN 0-7844-0553-0, Library of Congress Catalog Card No. 2001-018922, 2001, pp.590-604.

[5] Priestley, M.J.N., Verma, R., and Xiao, Y.: 'Seismic shear strength of reinforced concrete columns'. *ASCE, Journal of Structural Engineering,* 120(8), 1994, pp.2310-2329.

[6] Priestley, M.J.N., and Benzoni, G.: 'Seismic performance of circular columns with low longitudinal reinforcement ratios'. *ACI Structural Journal,* 93(4), 1996, pp.474-485.

[7] Hakuno, M., Shidawara, M., and Kara, T.: 'Dynamic destructive test of a cantilever beam controlled by an analog computer'. *Transaction of Japan Society of Civil Engineers,* No. 171, November 1-9, 1969.

[8] Tanzo, W., Yamada, Y., and Imeura, H.: 'Substructures computer-actuator hybrid loading tests for inelastic earthquake response of structures'. *Research Report No. 92-ST-01,* Kyoto University, Japan, 1992.

[9] Takanashi, K., et al.: 'Seismic failure analysis of structures by computer-pulsator on-line system'. *J. Inst. of Industrial Science,* 26(11), Univ. of Tokyo, 1974.

[10] Thewalt C., and Mahin S.: 'Hybrid solution techniques for generalized pseudo-dynamic testing'. Earthquake Engg. Research Center, Univ. of California, Berkeley [1987], *Report No. UCB/EERC-87109.* 1987.

[11] Shing P. S., and Mahin S. A.: 'Rate of loading effects on pseudo-dynamic tests'. *Journal of the Structural Division, ASCE,* V. 114, No. 11, Nov. 1988, pp.2403-2420.

[12] Priestley, M. J. N., Seible, F., and Chai, Y. H.: 'Design guidelines for assessment retrofit and repair of bridges for seismic performance'. *Report No. SSRP 92/01, Structural Systems Research Project,* University of California, San Diego, Feb. 1992, 226p.

[13] Seismic Design Code for Prestressed Concrete Structures (Draft), Japan Prestressed Concrete Engineering Association, Japan.

[14] Ang, B.G., Priestley, M.J.N., and Paulay, T.: 'Seismic shear strength of circular reinforced concrete columns'. *ACI Structural Journal:* 86(1), 1989, pp45-59.

[15] Yoshikawa, H., and Miyagi, T.: 'Ductility and failure modes of single reinforced concrete columns'. *Seminar on Post-peak Behavior of RC Structures Subjected to Seismic Loads:* Vol. 2, 1999, pp.229-244.

[16] Priestley, M.J.N., Seible, F., Xiao, Y., and Verma, R.: 'Steel jacket retrofitting of reinforced concrete bridge columns for enhanced shear strength-Part 1'. *ACI Structural Journal,* 1994.

[17] Priestley, M.J.N., Seible, F., Xiao, Y., and Verma, R.: 'Steel jacket retrofitting of reinforced concrete bridge columns for enhanced shear strength-Part 2'. *ACI Structural Journal,* 1994.